Cellulose (2016) 23:2863–2876
DOI 10.1007/s10570-016-0997-8

ORIGINAL PAPER

Per-*O*-acylation of xylan at room temperature in dimethylsulfoxide/*N*-methylimidazole

Xueqin Zhang · Aiping Zhang · Chuanfu Liu · Junli Ren

Received: 16 March 2016 / Accepted: 27 June 2016 / Published online: 15 July 2016

Abstract The per-*O*-acylation of xylan-type hemicellulose was firstly carried out in dimethylsulfoxide/*N*-methylimidazole (DMSO/NMI) at room temperature without additional catalyst. The optimum conditions for esterification of xylan was investigated in terms of the molar ratio of reagents to anhydroxylose units (AXU) in xylan and the kinds of esterification reagents to obtain a high degree of substitution (DS, 1.98) and weight percent gain (WPG, 86.88 %) of xylan esters. In this solvent system, NMI acted as a solvent, a base and an excellent catalyst, therefore, the per-*O*-acylation of xylan (DS of 1.98) was readily accomplished in DMSO/NMI system at room temperature. Structure elucidation of xylan esters was characterized by FT-IR and NMR (^{1}H-NMR, ^{13}C-NMR and HSQC). FT-IR and NMR analyses provided the direct evidence of per-*O*-acylation of xylan under the given conditions. Furthermore, HSQC revealed the higher reactivity of hydroxyls at C-2 position than those at C-3 position of xylan. The solubility of xylan in DMSO, DMF and $CHCl_3$ improved after esterification. TGA/DTG indicated that the thermal stability of xylan increased after the esterification with anhydrides, while decreased with acyl chlorides, probably due to degradation and hydrolysis of the acylated xylan at the presence of by-product hydrochloric acid.

Keywords Xylan · Per-*O*-acylation · DMSO/NMI · Room temperature

X. Zhang · C. Liu (✉) · J. Ren
State Key Laboratory of Pulp and Paper Engineering, South China University of Technology, Guangzhou 510640, People's Republic of China
e-mail: chfliu@scut.edu.cn

A. Zhang
College of Materials and Energy, Guangdong Key Laboratory for Innovative Development and Utilization of Forest Plant Germplasm, South China Agricultural University, Guangzhou 510642, People's Republic of China

Introduction

For the increasing depletion of non-renewable petrochemicals and concerns on the environmental problems, extensive attention has been conducted on conversion plant biomass as functional bio-polymeric materials for its excellent biodegradability, renewability and availability (Samuel et al. 2011; Alonso et al. 2013). Biomass has a complex structure consisting of three main polymeric components, cellulose (30–40 %), hemicelluloses (20–35 %) and lignin (15–25 %) (Saha 2003; Belmokaddem et al. 2011; Ruiz et al. 2013).

Hemicelluloses are defined as a group of heteropolysaccharides with low molecular weight and a degree of polymerization (DP) typically between 80 and 425 (Ayoub et al. 2013). Hemicelluloses occur in a large variety of structural types, divided into four

general groups: xylans, mannans, glucans and xyloglucans (Saha 2003; Belmokaddem et al. 2011). Xylan-type polysaccharides are the most abundant hemicelluloses and mainly consist of D-xylopyranose (D-xyl*p*) units in the backbone linked by β-(1 → 4) glycosidic bonds with 4-*O*-methyl-D-glucuronic acid (MeGlcA) and acetyl side groups (Saha 2003; Vega et al. 2012; Sundberg et al. 2015). In contrast of cellulose, for the inherent branched structure, low molecular weight and strong hydrophilicity, the potential utilization of hemicelluloses as starting materials for derivatization has not been fully explored.

Chemical modification can effectively substitute the free hydroxyl groups on macromolecules to compensate for the drawbacks and create the novel opportunities to exploit the various valuable properties of hemicelluloses (Liu et al. 2009; Enomoto Rogers and Iwata 2012; Zhang et al. 2014, 2015a). Among modification, esterification is one of the most versatile functionalization procedures that can be used in particular to improve the hydrophobicity, solubility and thermal processability of hemicelluloses (Wu et al. 2004; Yan et al. 2009; Fundador et al. 2012a). Traditionally, the researches of preparing hemicelluloses esters were mainly conducted in different solvents with various catalysts (Renard and Jarvis 1999; Gröndahl et al. 2003). For example, corn cob hemicelluloses esters with acid anhydride were prepared with catalyst of pyridine in formamide (Carson and Maclay 1948); a series of xylan acetates were obtained in dimethylacetamide (DMAc)/lithium chloride (LiCl)/pyridine system at 50 °C, and different degrees of substitution (DS) were obtained (Fundador et al. 2012a); xylan esters with varying alkyl chain lengths (C2–C12) were prepared in heterogeneous (trifluoro acetic anhydride/acid) and homogeneous (DMAc/LiCl/pyridine) reactions at 50 °C (Fundador et al. 2012b); aspen glucuronoxylan was acetylated with acetic anhydride in formamide and pyridine (Gröndahl et al. 2003); acetylated wheat straw hemicelluloses were prepared in ionic liquid 1-butyl-3-methylimidzolium chloride ([C_4mim]Cl) at 100 °C with iodine as catalyst, and DS ranged from 0.49 to 1.53 (Ren et al. 2007). However, these synthetic procedures with different catalysts and high reaction temperature were complicated and uneconomic. Therefore, in order to simplify the procedures as well as improve the properties of hemicelluloses derivatives, we make the attempt to perform derivatization reactions of hemicelluloses under the mildest conditions, in which the substitutions along the backbone can also be achieved with effective yields.

In recent years, dimethyl sulfoxide/*N*-methylimidazole (DMSO/NMI) was founded to be capable of dissolving lignocelluloses under relatively mild conditions without apparent degradation (Lu and Ralph 2003; Zhang et al. 2012). This suggested to us that DMSO/NMI may also be applied as an efficient reaction medium for the derivatization reactions of hemicelluloses. More importantly, NMI in this solvent system is an excellent acylation catalyst, so in situ acetylation is readily accomplished (Lu and Ralph 2003; Zhang et al. 2012). In this case, the esterification reactions of xylan–type hemicellulose could be achieved in DMSO/NMI with NMI as acylation catalyst, that is to say, without any additional catalysts. This can largely simplify the esterification procedures. The optimization of reaction parameters, including the molar ratio of reagents to anhydroxylose units (AXU) and the kinds of reagents, including acetic anhydride (Aa), propionic anhydride (Pa), butyric anhydride (Ba), acetyl chloride (Ac), propionyl chloride (Pc) and butyryl chloride (Bc), was investigated to improve the reaction efficiency [denoted as DS and weight percent gain (WPG)]. Structural elucidation of xylan and xylan esters based on FT-IR, ^{1}H- and ^{13}C-NMR, HSQC is discussed in this paper. Thermal properties and solubility behaviour were also studied.

Experimental

Materials

Xylan (isolated from sugarcane bagasse) with xylose content of over 85 % was purchased from Yuan-Ye Biological Technology Co., Ltd. (Shanghai, China). Aa, Pa, Ba, Ac, Pc and Bc with a purity of 99 % were provided by Sigma-Aldrich Co., LLC (Shanghai, China). DMSO, NMI and other chemicals were of analytical-reagent grade from Guangzhou Chemical Reagent Factory (Guangdong, China). DMSO was dried over CaH_2 for 12 h and subsequently distilled under reduced pressure before use. Other chemicals were directly used without further purification.

Homogenous esterification of xylan in DMSO/NMI

The xylan esters, denoted as XyAa, XyPa, XyBa, XyAc, XyPc and XyBc, were homogeneously prepared in DMSO/NMI at room temperature with esterifying agents Aa, Pa, Ba, Ac, Pc and Bc, respectively, according the following procedure. Dried xylan (0.11 g, 1.67 mmol of hydroxyl groups in xylan) was suspended in 10 mL of DMSO and 5 mL of NMI. The mixture was agitated with magnetic stirring at 100 °C for about 1 h under nitrogen atmosphere to obtain xylan solution. Then the mixture was cooled to room temperature, and the esterifying agents were added into the xylan solution, as listed in Table 1. After the required time, the mixture was purified by dialysis (cutoff = 3000 g mol^{-1}) against water to remove DMSO, NMI, unreacted esterifying agents and by-products, and then freeze dried. The products were weighted to determine the percentage of weight increase, expressed by WPG, according to the following equation:

$$\mathrm{WPG} = \frac{\mathrm{m2} - \mathrm{m1}}{\mathrm{m1}} \times 100\ \%$$

where WPG is the weight percent gain of xylan after esterification, m1 (g) is the weight of xylan regenerated in DMSO/NMI, and m2 (g) is the weight of modified xylan samples.

Solubility behavior

The solubility of regenerated and acylated xylan in DMSO, dimethylformamide (DMF) and chloroform ($CHCl_3$) was investigated. A certain amount of sample (10 mg) was added in 0.5 mL solvent and stirred at room temperature for 12 h. After the required time, the results were recorded.

Characterization

The functional groups and chemical structure of unmodified xylan and xylan esters were examined by FT-TR spectroscopy using a Bruker spectrophotometer (Tensor 27, Germany) from a KBr disc containing 1 % (w/w) finely ground samples in the range of 4000–400 cm^{-1}.

The ^{1}H-NMR, ^{13}C-NMR and HSQC spectra of unmodified xylan, regenerated xylan and xylan esters were recorded from 40 mg samples in 0.5 mL DMSO-d_6 on a Bruker Avance III 600 M spectrometer (Germany) with a 5 mm multinuclear probe. For the ^{1}H-NMR analysis, the detailed collecting and processing parameters were listed as follows: number of scans, 16; receiver gain, 31; acquisition time, 2.7263 s; relaxation delay, 1.0 s; pulse width, 12.5 s; spectrometer frequency, 600.17 MHz; and spectral width, 12,019.2 Hz. For the ^{13}C-NMR analysis, the detailed collecting and processing parameters were listed as follows: number of scans, 5000; receiver gain, 187; acquisition time, 0.9088 s; relaxation delay, 2.0 s; pulse width, 11.5 s; spectrometer frequency, 150.91 MHz; and spectral width, 36,057.7 Hz. For the HSQC analysis, the detailed collecting and processing parameters were listed as follows: number of scans, 16; receiver gain, 187; acquisition time, 0.1420 s; relaxation delay, 2.0 s; pulse width, 12.5 s; spectrometer frequency, 600.17/150.91 MHz; and spectral width, 7211.5/24,875.6 Hz.

The thermal stability of samples was performed by using thermogravimetric analysis (TGA) and derivative thermogravimetry (DTG) on a Q500 thermogravimetric analyzer (TA, USA). To eliminate the effect of water, all samples were dried at 105 °C for 12 h before characterization. The apparatus was continually flushed with nitrogen. The sample between 9 and 11 mg was heated from 30 to 600 °C at a heating rate of 10 °C/min.

Results and discussion

Optimum conditions for esterification reaction of xylan in DMSO/NMI

Homogeneous esterification of hemicelluloses had already been achieved (Sun et al. 2000; Belmokaddem et al. 2011; Zhang et al. 2011b). However, the required reaction conditions were complicated, e.g. with high reaction temperature or catalyst. In the present study, the esterification of xylan was carried out in DMSO/NMI at room temperature without additional catalyst to simplify the reaction procedures. The optimum conditions in terms of the molar ratio of reagents to AXU (from 0.5:1 to 8:1) and the kinds of reagents, including Aa, Pa, Ba, Ac, Pc and Bc, were investigated to obtain appropriate reaction efficiency (Table 1; Fig. 1). To better view the reactivity of reagents, the

Table 1 Detailed structural factors of xylan esters obtained under various conditions

Sample	Reagent	Reagent/AXU (mol/mol)	DS[a]	WPG[b] (%)	Solubility		
					DMSO	DMF	$CHCl_3$
1	Aa	0.5:1	0.37	16.29	++	+	–
2	Aa	1:1	0.58	31.56	++	+	–
3	Aa	1.5:1	1.17	40.06	++	+	+
4	Aa	2:1	1.28	46.61	++	++	+
5	Aa	2.5:1	1.59	57.31	++	++	++
6	Aa	3:1	1.63	59.04	++	++	++
7	Aa	4:1	1.87	62.27	++	++	++
8	Aa	8:1	1.98	72.93	++	++	++
9	Ac	0.5:1	0.34	0.99	++	+	–
10	Ac	1:1	0.39	−2.76	++	+	–
11	Ac	1.5:1	0.84	−9.01	++	+	+
12	Ac	2:1	1.14	−28.62	++	+	+
13	Ac	2.5:1	1.42	−20.61	++	++	++
14	Ac	3:1	1.59	−8.41	++	++	++
15	Ac	4:1	1.77	−4.97	++	++	++
16	Ac	8:1	1.72	−6.73	++	++	++
17	Pa	0.5:1	0.41	21.78	++	+	–
18	Pa	1:1	0.63	41.92	++	+	–
19	Pa	1.5:1	0.69	43.68	++	+	–
20	Pa	2:1	1.19	58.41	++	+	+
21	Pa	2.5:1	1.34	63.66	++	++	+
22	Pa	3:1	1.54	66.67	++	++	++
23	Pa	4:1	1.83	67.51	++	++	++
24	Pa	8:1	1.95	78.74	++	++	++
25	Pc	0.5:1	0.32	6.71	++	+	–
26	Pc	1:1	0.54	4.99	++	+	–
27	Pc	1.5:1	0.62	0.29	++	+	–
28	Pc	2:1	1.16	−15.48	++	+	+
29	Pc	2.5:1	1.33	−13.31	++	++	+
30	Pc	3:1	1.49	−3.57	++	++	++
31	Pc	4:1	1.76	5.71	++	++	++
32	Pc	8:1	1.74	3.16	++	++	++
33	Ba	0.5:1	0.41	31.39	++	+	–
34	Ba	1:1	0.58	52.85	++	+	–
35	Ba	1.5:1	0.79	57.99	++	+	+
36	Ba	2:1	1.33	63.98	++	++	+
37	Ba	2.5:1	1.49	67.67	++	++	++
38	Ba	3:1	1.75	71.36	++	++	++
39	Ba	4:1	1.84	85.02	++	++	++
40	Ba	8:1	1.96	86.88	++	++	++
41	Bc	0.5:1	0.22	15.87	++	+	–
42	Bc	1:1	0.48	14.82	++	+	–

Table 1 continued

Sample	Reagent	Reagent/AXU (mol/mol)	DS[a]	WPG[b] (%)	Solubility		
					DMSO	DMF	$CHCl_3$
43	Bc	1.5:1	0.65	8.27	++	+	–
44	Bc	2:1	1.28	−0.81	++	++	+
45	Bc	2.5:1	1.37	−0.29	++	++	+
46	Bc	3:1	1.68	4.78	++	++	++
47	Bc	4:1	1.76	14.27	++	++	++
48	Bc	8:1	1.69	10.91	++	++	++
49	Re-xylan				++	+	–

[a] The degree of substitution of xylan esters, calculated by ^{1}H-NMR

[b] The weight percent gain of xylan after the esterification with anhydrides and acyl chlorides

$^{++}$ Representing soluble, $^{+}$ representing swelling, $^{-}$ representing insoluble

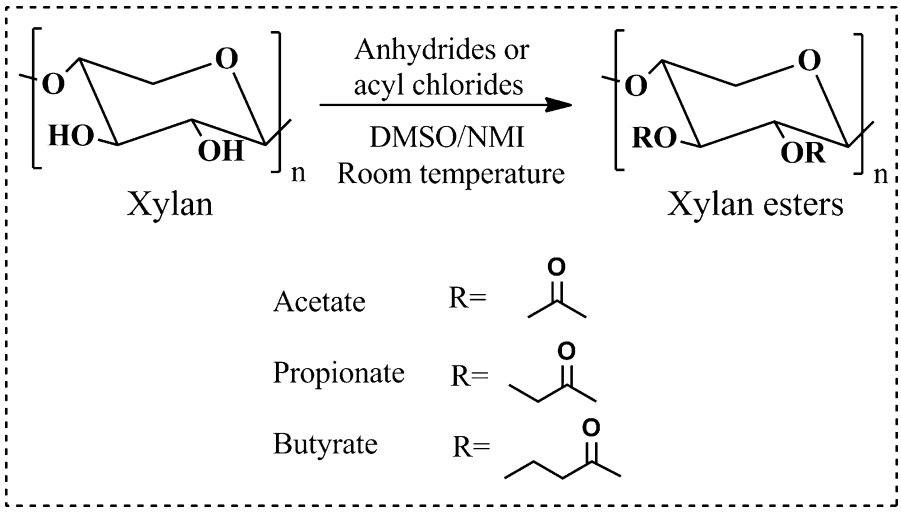

Fig. 1 Esterification of xylan with different reagents in DMSO/NMI at room temperature without additional catalyst

molar ratio of reagents in relation to DS and WPG is illustrated by graphical relation in Fig. 2.

Figure 2a illustrates the effect of the molar ratio of anhydrides to AXU on the DS of xylan esters (XyAa, XyPa and XyBa). Apparently, an increase of the molar ratio of anhydrides to AXU from 0.5:1 to 8:1 resulted in an increment in DS from 0.37 to 1.98 (XyAa), 0.41 to 1.95 (XyPa) and 0.41 to 1.96 (XyBa), respectively, indicating the favorable effect on xylan acylation. These results were probably due to the increased molecule collisions of acylation reagents with reactive hydroxyl groups in AXU. Theoretically, two hydroxyl groups are available to substitute at the position of C-2 and C-3 in each AXU of xylan, and the maximum DS is 2. Therefore, these results indicated that the per-*O*-acylation of xylan has readily accomplished in DMSO/NMI system at room temperature with the optimum molar ratio of anhydrides to AXU 8:1. More importantly, NMI is a derivative of imidazole with a slightly more basic *N*-methyl group as indicated by the pK_a's of the conjugate acids of 7.0 and 7.4 (Zhang et al. 2012). This means that NMI can act as a solvent, a base and an excellent acylation catalyst in DMSO/NMI solvent system (Lu and Ralph 2003; Liu et al. 2007; Zhang et al. 2012). Because the esterification of xylan with anhydride is acid- or base-catalyzed reaction, NMI shows promise in accelerating the esterification reaction. In comparison with DS, the WPG value displayed a similar trend as shown in Fig. 2b. An increase of the molar ratio of anhydrides to AXU from 0.5:1 to 8:1 resulted in an improvement of the WPG of XyAa, AyPa and XyBa from 16.29 to

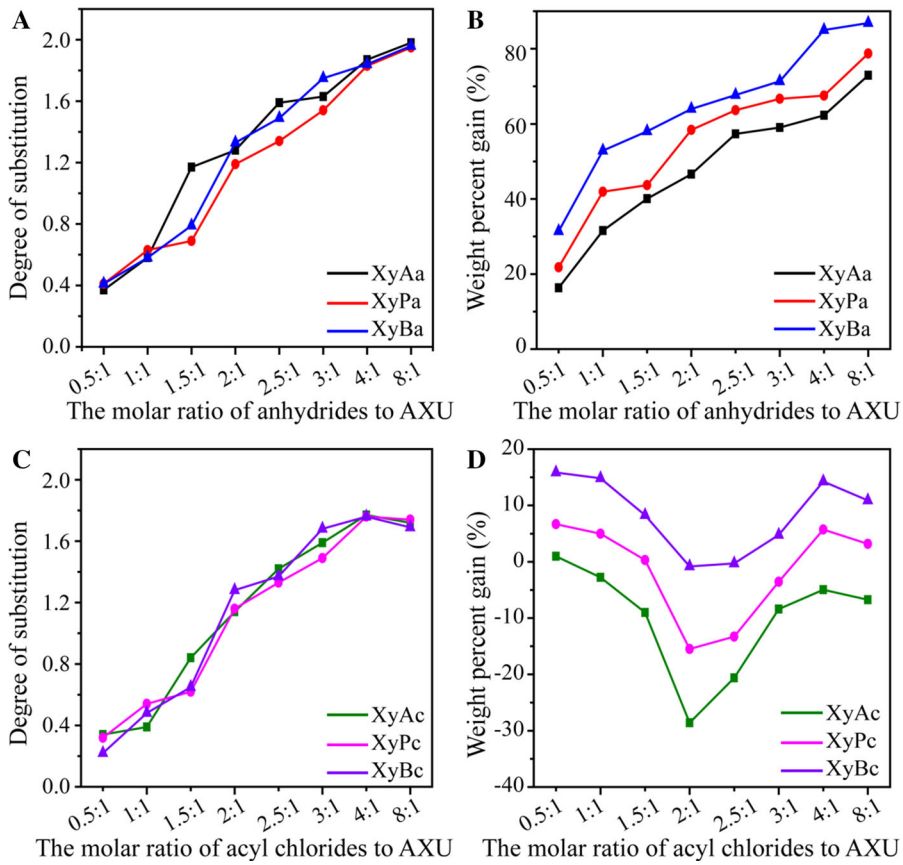

Fig. 2 The effects of the molar ratio of acylation reagents to AXU and the kinds of acylation reagents on the DS (**a**, **c**) and WPG (**b**, **d**) of xylan esters

72.93, 21.78 to 78.74 and 31.39 and 86.88 %, respectively.

Figure 2c, d show the influence of the molar ratio of acyl chlorides to AXU on the DS and WPG of xylan esters (XyAc, XyPc and XyBc). In general, DS of xylan esters gradually increased, then tapered and decreased after reaching the maximum value when increasing acyl chlorides dosages. From Fig. 2c, DS of XyAc, XyPc and XyBc increased from 0.34 to 1.77, 0.32 to 1.76 and 0.22 to 1.76, respectively, with increasing acyl chlorides dosages from 0.5:1 to 4:1. After reaching its optimum value, the DS of xylan esters decreased slightly with increasing acyl chlorides dosages from 4:1 to 8:1. These results indicated that higher molar ratio of acyl chlorides to AXU resulted in a decreased DS. This decrease in DS was probably due to the severe degradation and hydrolysis of the acylated xylan at the presence of the by-product hydrochloric acid (Zhang et al. 2012). In Fig. 2d, WPG of XyAc, XyPc and XyBc decreased from 0.99 to −28.62, 6.71 to −15.48 and 15.87 to −0.81 %, respectively, with the increase of the molar ratio of acyl chlorides from 0.5:1 to 2:1. This decrement was probably due to the degradation and hydrolysis of xylan esters at the presence of hydrochloric acid. Further increasing the reagents dosage from 2:1 to 4:1, and to 8:1 led to an increase in the WPG of XyAc, XyPc and XyBc from −28.62 to −4.97, −15.48 to 5.71 and −0.81 to 14.27 %, respectively, followed by a slight decrease. Therefore, these results showed that the condition that gave the maximum DS of XyAc, XyPc and XyBc was not same as that for the highest WPG. Due to the serious degradation of xylan esters caused by hydrochloric acid, the optimum conditions was selected mainly based on the highest DS. Therefore, the optimum molar ratio of acyl chlorides to AXU was 4:1.

In addition, Fig. 2 compares the influences of reagent species on the DS and WPG of xylan esters. Comparatively, when considering the value of DS and WPG of xylan esters, the reactivity of anhydrides was higher than acyl chlorides, which was probably due to the serious degradation of xylan esters caused by hydrochloric acid by-product. Figure 2 also presents

the effects of chain length (C2, C3 and C4) of anhydrides and acyl chlorides on DS and WPG of xylan esters. As shown in Fig. 2a, c, the DS values of xylan esters with anhydrides (Aa, Pa and Ba) and the corresponding acyl chlorides (Ac, Pc and Bc) were nearly equal, indicating the similar reactivity of anhydrides (Aa, Pa and Ba) and the corresponding acyl chlorides (Ac, Pc and Bc) under the selected conditions. Similar results were found in cellulose esters (Ratanakamnuan et al. 2012). In Fig. 2b, d, the noticeable differences of WPG increment of each xylan ester were observed with the increase of chain length of anhydrides and acyl chlorides, probably due to the attachment of acyl substituents (Ratanakamnuan et al. 2012). The longer acyl substituents represented the higher molecular weight of acyl group which can result in higher WPG of xylan derivatives [WPG XyBa (C4) > XyPa (C3) > XyAa (C2), XyBc (C4) > XyPc (C3) > XyAc (C2)].

In general, under the selected conditions, by varying reaction conditions, the DS (ranged from 0.22 to 1.98) and WPG (ranged from −28.62 to 86.88 %) of xylan derivatives could be selectively controlled, thus allowed the properties of the xylan derivatives to be tuned for use in various industrial applications. The optimum conditions for esterification of xylan with various reagents were varied, as summarized below: (1) the optimum dosage of anhydrides and acyl chlorides for maximum DS were 8:1 (XyAa, XyPa and XyBa) and 4:1 (XyAc, XyPc and XyBc), respectively; (2) the optimum dosage of anhydrides and acyl chlorides for maximum WPG were 8:1 (XyAa, XyPa and XyBa) and 0.5:1 (XyAc, XyPc and XyBc), respectively; (3) the reactivity of anhydrides and acyl chlorides were Aa > Ac, Pa > Pc and Ba > Bc, respectively; (4) the effects of chain length of anhydrides and acyl chlorides on the value of WPG were XyBa (C4) > XyPa (C3) > XyAa (C2) and XyBc (C4) > XyPc (C3) > XyAc (C2), respectively. It should be noted that NMI in this system acts as a solvent, a base as well as a catalyst, resulting in the achievement of the simplified and economical per-*O*-acylation of xylan at room temperature without additional catalyst. This is considered to be one of the important highlights of this research.

Solubility

One of the reasons that limits the application of most polysaccharides is their poor solubility in organic solvents (Fundador et al. 2012b). Esterification is one method to solve this problem, for the introduced hydrophobic acyl group can alter the chemical structure of the polysaccharides.

In this study, the solubility of esterified xylan in various organic solvents was investigated and the results are summarized in Table 1. It was found that the regenerated xylan (re-xylan) was swollen in DMF and insoluble in $CHCl_3$, probably due to the strong intermolecular hydrogen bonds between xylan chains. As expected, xylan esters with different DS could be easily dissolved in DMSO, providing the further structural characterization of the xylan derivatives with NMR. The solubility of xylan esters in DMF and $CHCl_3$ increased with an increase of DS. Similar results can also be observed in acylated cellulose (Fundador et al. 2012a; Ratanakamnuan et al. 2012). In general, the introduction of hydrophobic acyl groups into the molecular structure of xylan results in the destruction of hydrogen bonds, which was expected to improve its solubility.

FT-IR

FT-IR spectroscopy is the most convenient method for the elucidation of functional groups and structural features of xylan derivatives. Figure 3 compares the FT-IR spectra of unmodified xylan and xylan esters XyAa7 (DS = 1.87), XyPa23 (DS = 1.83) and XyBa39 (DS = 1.84). As shown in the spectrum of unmodified xylan, a sharp band at 898 cm^{-1} is

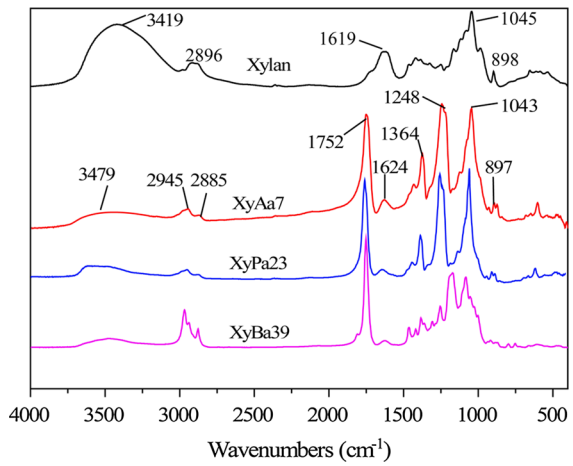

Fig. 3 FT-IR spectra of unmodified xylan and xylan esters XyAa7 (DS = 1.87), XyPa23 (DS = 1.83) and XyBa39 (DS = 1.84)

characteristic of β-glucosidic linkages between the sugar units (Fang et al. 1999; Belmokaddem et al. 2011). The band at 1045 cm^{-1} is assigned to C–O stretching in C–O–C linkages. An intense band at 1619 cm^{-1} corresponding to the adsorbed water is broader because it obscures vibrations of uronic acid carboxyl, which decreased substantially in xylan esters (Kačuráková et al. 2000). The bands at 3419 and 2896 cm^{-1} are attributed to hydrogen bond in hydroxyl groups (O–H) and the symmetric C–H vibration band, respectively. As can be seen, the spectra of XyAa7 (DS = 1.87), XyPa23 (DS = 1.83) and XyBa39 (DS = 1.84) provide evidence of acylation by the presence of three important typical ester bands at 1752 cm^{-1} (C=O ester), 1364 cm^{-1} (–C–CH_3) and 1248 cm^{-1} (C–O stretching) (Sun and Hughes 1999; Ayoub et al. 2013). The occurrence of peaks at around 2800–3000 cm^{-1} in the spectra indicates the presence of methyl and methylene C–H stretching of alkyl chains in xylan esters (Belmokaddem et al. 2011). As the carbon chain length of the acyl group increases from three-carbon chain (spectrum of XyPa23) to four-carbon chain (spectrum XyBa39), the signals of methyl and methylene band at around 2800–3000 cm^{-1} become intense. The O–H stretching vibration of xylan esters drifted from low wavenumber domain to 3479 cm^{-1}, probably due to the decrease of hydrogen bonding in xylan after esterification. Moreover, in comparison a drastic decrease was observed in the O–H stretching (3479 cm^{-1}), indicating the high degree of acylation of xylan, which was in accordance with the DS of xylan esters. Similar results were reported in acetylated cellulose (Chen et al. 2014).

According to previous studies, FT-IR spectra can provide an alternative method for calculating the DS (Samios et al. 1997; Zhang et al. 2011a; Chen et al. 2014). In the present study, a typical example of the detailed relationship between the DS of XyPa and the ratio of the hydroxyl peak (3479 cm^{-1}) height to the carbonyl peak (1752 cm^{-1}) area is presented in Table 2. From the data, the graph of the ratio of the peaks versus the DS was plotted (Fig. 4). This serves as a calibration curve from which the DS of other xylan esters can be calculated once the FT-IR spectrum is available. Thus, it can also be used as an alternative measurement to evaluate the DS of xylan esters obtained from ^{1}H-NMR spectra.

Table 2 The ratio of O–H (peak height) over C=O (peak area) for XyPa with different DS calculated from the FT-IR spectra

Sample	Reagent	DS	$A^a_{C=O}$	H^b_{OH}	$H_{OH}/A_{C=O} \times 10^3$
19	Pa	0.69	196.51	0.35	2.03
20	Pa	1.19	179.34	0.31	1.78
21	Pa	1.34	281.26	0.57	1.73
22	Pa	1.54	149.28	0.25	1.67
23	Pa	1.83	173.35	0.28	1.62
24	Pa	1.95	121.02	0.19	1.57

[a] Area of the band at 1752 cm^{-1} for C=O stretching

[b] Height of the band at 3479 cm^{-1} for O–H stretching

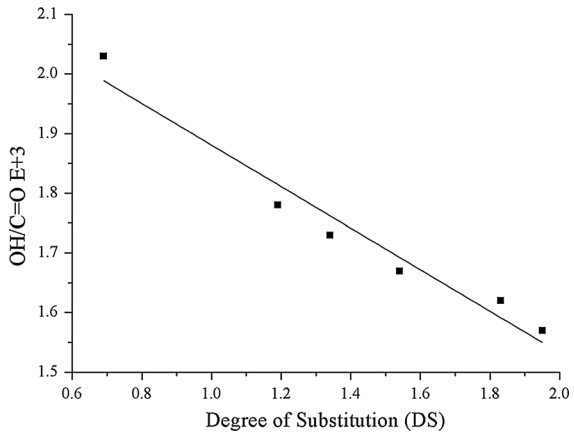

Fig. 4 Correlation between the DS of XyPa and the ratio of O–H (peak height, 3479 cm^{-1}) over C=O (peak area, 1752 cm^{-1})

NMR

In the present study, to elucidate the changes of xylan structure after acylation, the samples of unmodified xylan, XyAa7 (DS = 1.87), XyPa23 (DS = 1.83) and XyBa39 (DS = 1.84) were characterized with ^{1}H-NMR, ^{13}C-NMR and HSQC spectroscopies.

Figure 5 illustrates the ^{1}H-NMR (Left column) and ^{13}C-NMR spectra (Right column) of native xylan (A and B), XyAa7 (C and D, DS = 1.87), XyPa23 (E and F, DS = 1.83) and XyBa39 (G and H, DS = 1.84), respectively. In Fig. 5a, the β-(1 → 4)-linked D-xyl*p* units were characterized by the signals at 3.04, 3.32, 3.48, 9.91, 4.09 and 4.34 ppm, which correspond to the protons at H-2, H-5a, H-3, H-4, H-5e and H-1 of AXU in xylan, respectively (Fundador et al. 2012a;

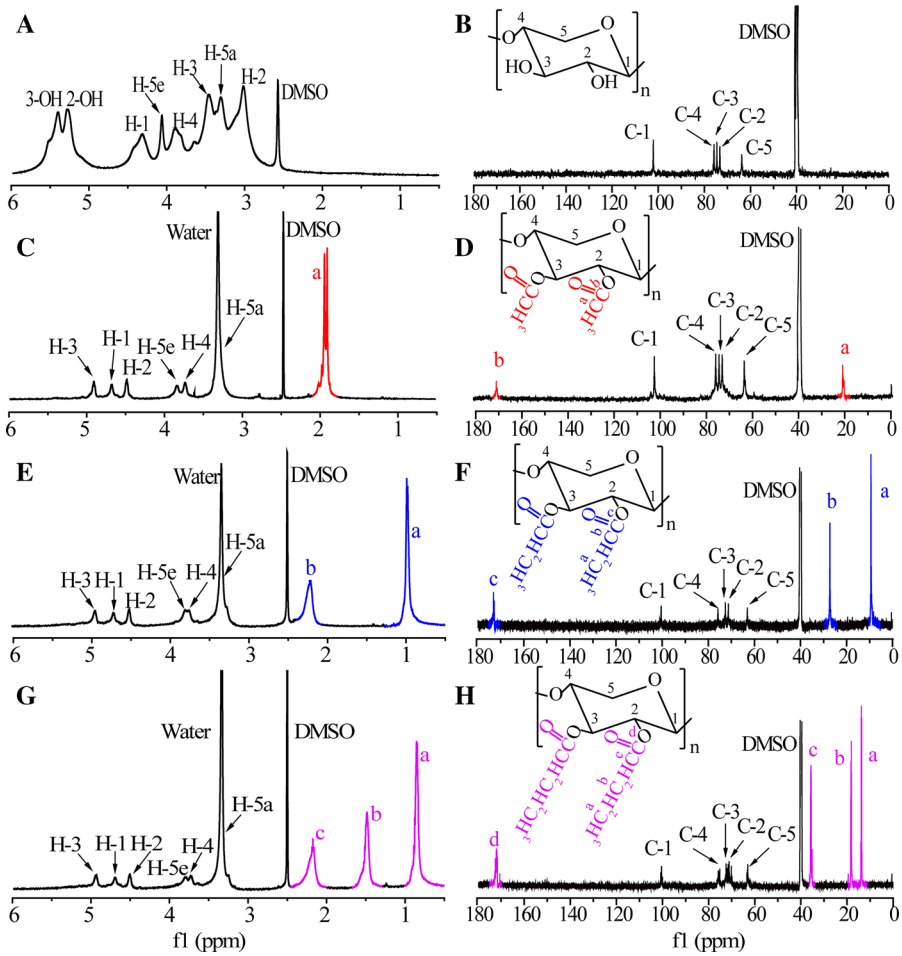

Fig. 5 ^{1}H-NMR (*left column*) and ^{13}C-NMR spectra (*right column*) of unmodified xylan (**a**, **b**), XyAa7 (**c**, **d**, DS = 1.87), XyPa23 (**e**, **f**, DS = 1.83) and XyBa39 (**g**, **h**, DS = 1.84), respectively

Zhang et al. 2015a). The proton signals at 5.29 and 5.41 ppm are assigned to the hydroxyl groups (2-OH and 3-OH) in xylan. In addition, the signals at 3.60, 3.78, 3.91 and 3.41 are attributed to H-2, H-3, H-4 and H-5 in α-L-arabinofuranosyl residues (α-L-Ara*f*) (Wen et al. 2011). The signal at 5.25 ppm in the ^{1}H-NMR spectrum has been assigned to protons at C-1 of MeGlcA residues. However, the signal corresponding to the protons of the acetyl groups at about 1.90 ppm was not observed, probably for its low content or the isolated method (Fundador et al. 2012b). In Fig. 5c (XyAa7, DS = 1.87), the signal at 1.95 ppm relates to the hydrogen proton in methyl group (–C$\underline{H}_3$) from the attached acyl moieties. This result confirms the successful esterification of xylan. In addition, the signals at 3.26, 3.75, 3.85, 4.51, 4.68 and 4.92 ppm are attributed to H-5a, H-4, H-5e, H-2, H-1 and H-3 of the ring structure of XyAa7, respectively. In terms of XyPa23 (Fig. 5e), the signals assigning to the acyl moieties a and b are located in 0.97 and 2.20 ppm, respectively. For XyBa39 (Fig. 5g), the signals at 0.84, 1.48 and 2.17 ppm are corresponded to the acyl moieties a, b and c, respectively. The signals in the range of 3.00 to 5.50 ppm are attributed to the ring protons in AXU backbone. It should be noted that, the signals corresponding to the protons of the hydroxyl groups attached at C-2 (2-OH) and C-3 (3-OH) in AXU could not be detected in xylan esters, indicating their high DS (Fundador et al. 2012b; Zhang et al. 2015b).

On the basis of the typical proton signals from xylan esters, the DS of xylan esters (Table 1) was calculated according to the following equation (Belmokaddem et al. 2011):

$$DS = \frac{I_a/3}{(I_{H1} + I_{H4})/2}$$

where DS is the degree of substitution of xylan esters, I_a is the integral area of the resonances of the methyl protons at a, I_{H1} and I_{H4} are the integral areas of anomeric proton assigned to H-1 and H-4 of AXU.

Figure 5 also lists the ^{13}C-NMR spectra of xylan and xylan esters. In ^{13}C-NMR spectrum of unmodified xylan (Fig. 5b), the five major signals at 63.7, 73.2, 74.5, 75.8 and 102.1 ppm are attributed to C-5, C-2, C-3, C-4 and C-1 of xylan, respectively. Similar findings were observed with other xylan sources (Wen et al. 2011; Fundador et al. 2012b; Vega et al. 2012). However, the signals attributing to acetyl groups, MeGlcA and other sugar residues were not detected, probably due to their low content in xylan. The ^{13}C-NMR spectra of the xylan esters are displayed in Fig. 5d, f, h. In Fig. 5d (XyAa7, DS = 1.87), the signals for the ring structure of xylan were detected. In addition, the signals at 26.6 and 172.9 ppm originate from the –$\underline{C}H_3$ (methyl, a) and $\underline{C}$=O (carbonyl, b) in the acyl moieties. In Fig. 5f (XyPa23, DS = 1.83), the signals at 9.4, 27.2 and 172.8 ppm are attributed to a (–$\underline{C}H_3$, methyl), b (–$\underline{C}H_2$–, methylene) and c ($\underline{C}$=O, carbonyl) of the acyl moieties, respectively (Fundador et al. 2012b). In case of Fig. 5h (XyBa39, DS = 1.84), the signals at 171.8 ($\underline{C}$=O, d), 35.2 (–$\underline{C}H_2$–, methylene, c), 18.3 (–$\underline{C}H_2$–, methylene, b) and 13.6 ppm (methyl, –$\underline{C}H_3$, a) in acyl moieties of esters side chains are all observed. These signals further supported the data, indicating the successful esterification of xylan.

HSQC is an efficient tool for qualitative and quantitative characterization of chemical structures, and can provide more detailed information about the signals which was overlapped in ^{1}H- and ^{13}C-NMR. To better understand the chemical structure of xylan and xylan esters, Fig. 6 represents the HSQC spectra of unmodified xylan (A), regenerated xylan (B), XyPc31 (C, DS = 1.76) and XyBa39 (D, DS = 1.84), and the different correlations from xylan backbone, sugar residues and esters side chains are exhibited in Red, Green and Blue, respectively. In Fig. 6a, the six strong correlations (presented in Red) at δ_C/δ_H 102.1/4.26, 73.2/3.02, 74.5/3.25, 75.8/3.48, 63.7/3.85 and 63.7/3.13 ppm are related to C_1–H_1, C_2–H_2, C_3–H_3, C_4–H_4, C_{5e}–H_{5e} and C_{5a}–H_{5a}, respectively, in xylan backbone. The four correlations (presented in Green) at δ_C/δ_H 78.3/3.60, 80.8/3.78, 86.4/3.91 and 62.2/3.41 ppm are attributed to C_2–H_2, C_3–H_3, C_4–H_4 and C_5–H_5 in α-L-Ara*f* (Wen et al. 2011). The presence of MeGlcA was characterized by the weak correlation at δ_C/δ_H 107.7/5.25 ppm corresponding to C_1–H_1 methoxy proton (presented in Green) (Belmokaddem et al. 2011). As shown in the HSQC spectrum of regenerated xylan (Fig. 6b), the major signals corresponded to xylan backbone, α-L-Ara*f* and MeGlcA were also detected, indicating that DMSO/NMI was capable of dissolving xylan without apparent degradation. As shown in Fig. 6c (XyPc31, DS = 1.76), the correlations which are found at δ_C/δ_H 9.1/0.98 and 27.3/2.21 ppm arise from the protons in the acyl moieties specifically from the methyl protons (–CH_3, C_a–H_a) and methylene (–CH_2–, C_b–H_b), respectively. These results confirm the successful esterification of xylan in DMSO/NMI. Moreover, the six strong correlations at δ_C/δ_H of 100.3/4.70, 71.0/4.54, 72.3/4.97, 76.1/3.76, 62.7/3.27 and 62.7/3.80 ppm are assigned to C_1–H_1, C_2–H_2, C_3–H_3, C_4–H_4, C_{5a}–H_{5a} and C_{5e}–H_{5e} in AXU, respectively. In Fig. 6d, the correlations at δ_C/δ_H 13.7/0.87, 18.1/1.50 and 35.9/2.18 ppm are corresponded to C_a–H_a (–CH_3), C_b–H_b (–CH_2–) and C_c–H_c (–CH_2–) in acyl moieties of XyBa39. The correlations for the ring structure of XyBa39 were also clearly detected. Apparently, more esters were attached to C_2 position than to C_3 position in AXU backbone. The results of integrated resonances indicated that 50.76/49.24 % (XyBa39, DS = 1.84) and 51.23/48.77 % (XyPc31, DS = 1.76) were attached to C_2 and C_3 positions of AXU, respectively. Note that, the correlations arising from MeGlcA and α-L-Ara*f* residues were not detected in XyPc31 and XyBa39. This is probably due to the formation of carboxylic acid or hydrochloric acid by-products in esterification reactions resulting in the decrease of these sugar residues in xylan esters, which could not be observed in HSQC spectra. In addition, in comparison with xylan derivatives with low DS (Zhang et al. 2014), the correlations for substituted C_2–H_2 and C_3–H_3 could not be detected in xylan esters with high DS, indicating the reliability of DS calculation on the basis of ^{1}H-NMR.

TGA/DTG

TGA/DTG analysis provide information on the thermal decomposition profiles of derivatives, which can be used to follow the physiochemical changes that

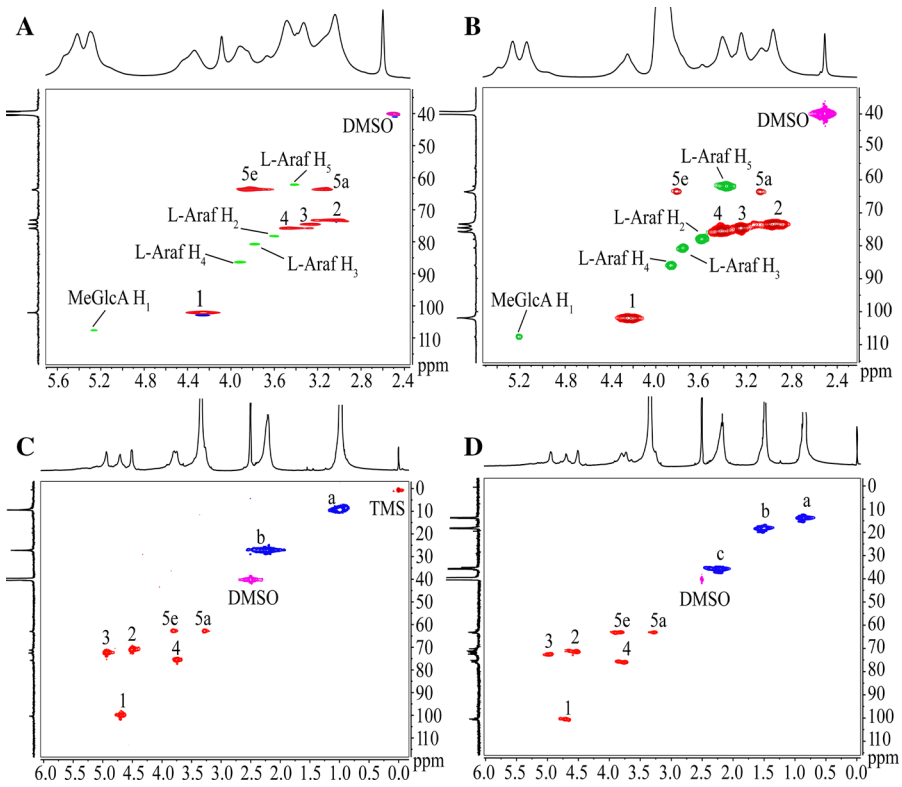

Fig. 6 HSQC spectra of unmodified xylan (**a**), regenerated xylan (**b**), xylan esters XyPc31 (**c**, DS = 1.76) and XyBa39 (**d**, DS = 1.84)

occur during chemical modification (El-Sayed and Mostafa 2014). Moreover, thermal stability of derivatives is an important parameter in exploring its further applications (Yan et al. 2009). Therefore, TGA/DTG was applied to investigate the effects of DS and esterifying reagents on the thermal stability of xylan esters. Figure 7 shows a comparison of the thermal properties of xylan and xylan esters (XyPa17, XyPa23, XyPc25 and XyPc31) with different DS. As shown in TGA curves, the onset of degradation takes place at about 150, 160, 180, 200, 220 °C for XyPc25, XyPc31, xylan, XyPa17 and XyPa23, respectively. The temperature at which there is 10 % w/w weight loss is about 200, 210, 230, 240 and 250 °C for XyPc25, XyPc31, xylan, XyPa17 and XyPa23, respectively. As can be seen, the thermal stability is

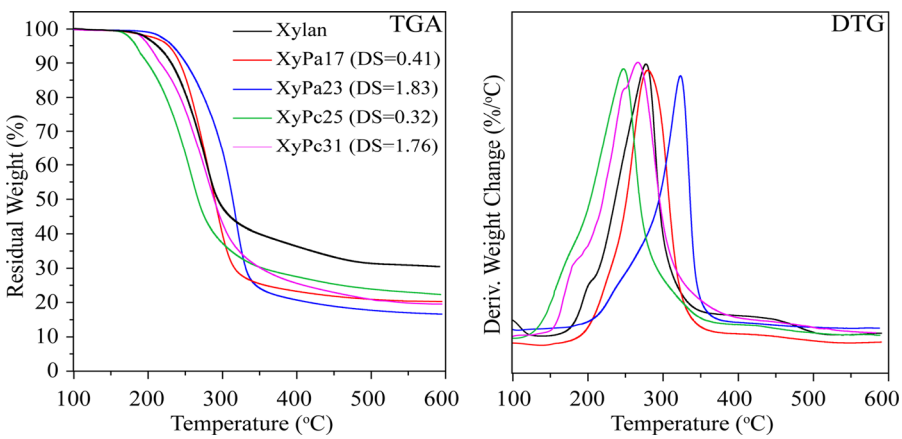

Fig. 7 TGA/DTG curves of unmodified xylan and xylan esters with different DS

improved by acylation with anhydrides while decreased with acyl chlorides. The high thermal stability of XyPa is brought about by the decrease in the number of remaining hydroxyl groups after esterification (Aburto et al. 1999; Fundador et al. 2012a). Similar findings were observed with other xylan esters (Belmokaddem et al. 2011; Fundador et al. 2012b). In previous study, the thermal stability of xylan esters with decanoyl chloride and lauroyl chloride was higher than unmodified xylan (Fundador et al. 2012b). However, in the present study, the thermal stability of xylan decreased after the esterification with acyl chloride, which was probably due to the shorter alkyl chain length and the serious degradation of xylan esters for the formation of hydrochloric acid (Fundador et al. 2012b). At the end of the analysis, it was noted that xylan esters had lower residual weight compared to unmodified xylan, probably due to the decreased contents of inorganic salts after the esterification in DMSO/NMI. Similar findings were observed with acetylated xylans in DMF (Belmokaddem et al. 2011).

Figure 7 also represents the DTG curves of samples. The DTG curves show the weight loss rates, and DTG_{max} presents the maximum degradation rate to compare the thermal stability between samples (Nadji et al. 2009). In DTG curves, the DTG_{max} are determined at about 270, 275, 320, 250 and 265 °C for the unmodified xylan, XyPa17, XyPa23, XyPc25 and XyPc31, respectively, which implied that the thermal stability of xylan increased after esterification with anhydride, while decreased with acyl chloride. This is probably for the serious degradation of xylan esters in the presence of hydrochloric acid by-product. Generally, esterification is an effective method to improve the thermal processability of xylan, which could broaden its applications, like blend with other polymers to produce thermoplastics.

Conclusions

In this study, xylan-type hemicellulose was successfully transformed into xylan derivatives through esterification with acetic anhydride, propionic anhydride, butyric anhydride, acetyl chloride, propionyl chloride and butyryl chloride as esterifying agents in dimethylsulfoxide/*N*-methylimidazole (DMSO/NMI) at room temperature. NMI in this system acted as a solvent, a base and a catalyst, which largely simplified the esterification of xylan. The optimum conditions were investigated by degree of substitution (DS) and weight percent gain (WPG) in terms of the molar ratio of reagents to anhydroxylose units (AXU) and the kinds of reagents. The results indicated that the DS and WPG of xylan esters acylated with anhydrides increased with increasing the dosage of acylation reagents, thus obtained per-*O*-acylated xylan with DS of 1.98 (the molar ratio of acetic anhydride to AXU was 8:1) and maximum WPG of 86.88 % (the molar ratio of butyric anhydride to AXU was 8:1), respectively. In comparison the lower DS and WPG of xylan esters acylated with acyl chlorides was probably due to the formation of hydrochloric acid leading the degradation of xylan esters. Solubility results indicated the increased solubility of xylan esters in organic solvents like DMSO, DMF and $CHCl_3$, which could broaden its applications. FT-IR and NMR were conducted to elucidate the structural features of xylan esters. HSQC suggested that 51.23/48.77 % (XyPc31, DS = 1.76) and 50.76/49.24 % (XyBa39, DS = 1.84) of esters were attached to C_2 and C_3 positions of AXU, respectively. TGA/DTG analysis illustrated that the thermal stability of xylan increased upon esterification with acid anhydrides, while decreased with acyl chlorides. Future works will be conducted on the application of these xylan esters.

Acknowledgments This work was financially supported by the National Natural Science Foundation of China (31170550, 31170555), Program for New Century Excellent Talents in University (NCET-11-0154), the Fundamental Research Funds for the Central Universities, and National Program for Support of Top-notch Young Professionals.

References

Aburto J, Alric I, Thiebaud S, Borredon E, Bikiaris D, Prinos J, Panayiotou C (1999) Synthesis, characterization, and biodegradability of fatty-acid esters of amylose and starch. J Appl Polym Sci 74(6):1440–1451

Alonso DM, Wettstein SG, Mellmer MA, Gurbuz EI, Dumesic JA (2013) Integrated conversion of hemicellulose and cellulose from lignocellulosic biomass. Energy Environ Sci 6(1):76–80

Ayoub A, Venditti RA, Pawlak JJ, Sadeghifar H, Salam A (2013) Development of an acetylation reaction of switchgrass hemicellulose in ionic liquid without catalyst. Ind Crop Prod 44:306–314

Belmokaddem F-Z, Pinel C, Huber P, Petit-Conil M, Da Silva Perez D (2011) Green synthesis of xylan hemicellulose esters. Carbohydr Res 346(18):2896–2904

Carson JF, Maclay WD (1948) Esters of lima bean pod and corn cob hemicelluloses. J Am Chem Soc 70(1):293–295

Chen CY, Chen MJ, Zhang XQ, Liu CF, Sun RC (2014) Per-*O*-acetylation of cellulose in dimethyl sulfoxide with catalyzed transesterification. J Agric Food Chem

El-Sayed SA, Mostafa ME (2014) Pyrolysis characteristics and kinetic parameters determination of biomass fuel powders by differential thermal gravimetric analysis (TGA/DTG). Energ Convers Manag 85:165–172

Enomoto Rogers Y, Iwata T (2012) Synthesis of xylan-graft-poly(L-lactide) copolymers via click chemistry and their thermal properties. Carbohydr Polym 87(3):1933–1940

Fang JM, Sun R, Fowler P, Tomkinson J, Hill CAS (1999) Esterification of wheat straw hemicelluloses in the N, N-dimethylformamide/lithium chloride homogeneous system. J Appl Polym Sci 74(9):2301–2311

Fundador NGV, Enomoto-Rogers Y, Takemura A, Iwata T (2012a) Acetylation and characterization of xylan from hardwood kraft pulp. Carbohydr Polym 87(1):170–176

Fundador NGV, EnomotoRogers Y, Takemura A, Iwata T (2012b) Syntheses and characterization of xylan esters. Polymer 53(18):3885–3893

Gröndahl M, Teleman A, Gatenholm P (2003) Effect of acetylation on the material properties of glucuronoxylan from aspen wood. Carbohydr Polym 52(4):359–366

Kačuráková M, Capek P, Sasinková V, Wellner N, Ebringerová A (2000) FT-IR study of plant cell wall model compounds: pectic polysaccharides and hemicelluloses. Carbohydr Polym 43(2):195–203

Liu BK, Wu Q, Xu JM, Lin XF (2007) *N*-methylimidazole significantly improves lipase-catalysed acylation of ribavirin. Chem Commun 3:295–297

Liu CF, Zhang AP, Li WY, Yue FX, Sun RC (2009) Homogeneous modification of cellulose in ionic liquid with succinic anhydride using *N*-bromosuccinimide as a catalyst. J Agric Food Chem 57(5):1814–1820

Lu FC, Ralph J (2003) Non-degradative dissolution and acetylation of ball-milled plant cell walls: high-resolution solution-state NMR. Plant J 35(4):535–544

Nadji H, Diouf PN, Benaboura A, Bedard Y, Riedl B, Stevanovic T (2009) Comparative study of lignins isolated from Alfa grass (*Stipa tenacissima* L.). Bioresour Technol 100(14):3585–3592

Ratanakamnuan U, Atong D, Aht-Ong D (2012) Cellulose esters from waste cotton fabric via conventional and microwave heating. Carbohydr Polym 87(1):84–94

Ren JL, Sun RC, Liu CF, Cao ZN, Luo W (2007) Acetylation of wheat straw hemicelluloses in ionic liquid using iodine as a catalyst. Carbohydr Polym 70(4):406–414

Renard CMGC, Jarvis MC (1999) Acetylation and methylation of homogalacturonans 1: optimisation of the reaction and characterisation of the products. Carbohydr Polym 39(3):201–207

Ruiz HA, Cerqueira MA, Silva HD, Rodriguez-Jasso RM, Vicente AA, Teixeira JA (2013) Biorefinery valorization of autohydrolysis wheat straw hemicellulose to be applied in a polymer-blend film. Carbohydr Polym 92(2):2154–2162

Saha B (2003) Hemicellulose bioconversion. J Ind Microbiol Biotechnol 30(5):279–291

Samios E, Dart RK, Dawkins JV (1997) Preparation, characterization and biodegradation studies on cellulose acetates with varying degrees of substitution. Polymer 38(12):3045–3054

Samuel R, Foston M, Jiang N, Allison L, Ragauskas AJ (2011) Structural changes in switchgrass lignin and hemicelluloses during pretreatments by NMR analysis. Polym Degrad Stab 96(11):2002–2009

Sun RC, Hughes S (1999) Fractional isolation and physicochemical characterization of alkali-soluble polysaccharides from sugar beet pulp. Carbohydr Polym 38(3):273–281

Sun R, Fang JM, Tomkinson J (2000) Stearoylation of hemicelluloses from wheat straw. Polym Degrad Stab 67(2):345–353

Sundberg J, Toriz G, Gatenholm P (2015) Effect of xylan content on mechanical properties in regenerated cellulose/xylan blend films from ionic liquid. Cellulose 22(3):1943–1953

Vega B, Petzold-Welcke K, Fardim P, Heinze T (2012) Studies on the fibre surfaces modified with xylan polyelectrolytes. Carbohydr Polym 89(3):768–776

Wen JL, Xiao LP, Sun YC, Sun SN, Xu F, Sun RC, Zhang XL (2011) Comparative study of alkali-soluble hemicelluloses isolated from bamboo (*Bambusa rigida*). Carbohydr Res 346(1):111–120

Wu J, Zhang J, Zhang H, He J, Ren Q, Guo M (2004) Homogeneous acetylation of cellulose in a new ionic liquid. Biomacromolecules 5(2):266–268

Yan C, Zhang J, Lv Y, Yu J, Wu J, Zhang J, He J (2009) Thermoplastic cellulose-graft-poly(L-lactide) copolymers homogeneously synthesized in an ionic liquid with 4-dimethylaminopyridine catalyst. Biomacromolecules 10(8):2013–2018

Zhang K, Feldner A, Fischer S (2011a) FT Raman spectroscopic investigation of cellulose acetate. Cellulose 18(4):995–1003

Zhang XM, Meng LY, Xu F, Sun RC (2011b) Pretreatment of partially delignified hybrid poplar for biofuels production: characterization of organosolv hemicelluloses. Ind Crop Prod 33(2):310–316

Zhang AP, Liu CF, Sun RC, Xie J, Chen XY (2012) Homogeneous acylation of eucalyptus wood at room temperature in dimethyl sulfoxide/*N*-methylimidazole. Bioresour Technol 125:328–331

Zhang XQ, Chen MJ, Liu CF, Sun RC (2014) Dual-component system dimethyl sulfoxide/LiCl as a solvent and catalyst for homogeneous ring-opening grafted polymerization of ε-caprolactone onto xylan. J Agric Food Chem 62(3):682–690

Zhang XQ, Chen MJ, Liu CF, Zhang AP, Sun RC (2015a) Homogeneous ring opening graft polymerization of ε-caprolactone onto xylan in dual polar aprotic solvents. Carbohydr Polym 117:701–709

Zhang XQ, Chen MJ, Liu CF, Zhang AP, Sun RC (2015b) Ring-opening graft polymerization of propylene carbonate onto xylan in an ionic liquid. Molecules 20:6033–6047